Supporting Information

for

The Rational Inclusion of Vitamin B_6 Boosts Artificial Cobalt Complex Catalyzed Green H_2 Production

Ab Qayoom Mir[b*†], Sukanta Saha[a†], Sampurna Mitra [a], Somnath Guria[b], Piyali Majumder[a], Dependu Dolui[a*], Arnab Dutta[a,c*]

[a]Chemistry Department, Indian Institute of Technology, Bombay, Maharashtra, India-400076.

[b]Discipline of Chemistry, Indian Institute of Technology, Gandhinagar, Gujarat, India-382355.

[c]Interdisciplinary Program Climate Studies, Indian Institute of Technology, Bombay, Maharasthra, India-400076

[†]These authors have contributed equally

* Corresponding author ab.qayoom@alumni.iitgn.ac.in, dolui.iitb@gmail.com, arnab.dutta@iitb.ac.in

Table of Contents

1. Materials and Methods:

Reagents were purchased from commercially available sources, and were used without any further purification. Millipore water (18.2 MΩ.cm at 298K) was used for all the studies and analysis. Optical absorption spectra were recorded on JASCO V-750 spectrometers using 1 cm path length. FTIR spectra of the solid complexes were recorded on the Perkin Elmer (Spectrum-Two) instrument. Nuclear Magnetic Resonance Spectra (NMR) were recorded at ~300K temperature using a Bruker Avance III 500 MHz Ascent FT spectrometer with working frequencies of 500 MHz for ^{1}H and 125 MHz for ^{13}C nuclei. Cyclic voltammetry (CV) studies were carried out using Metrohm Auto lab PGSTAT 201 potentiostat. The measurements were carried out in aqueous buffer using 0.1M 2-(N-Morpholino)ethane sulfonic acid, hydrate (MES) in millipore water, using 0.1M anhydrous sodium sulphate as supporting electrolyte. During the electrochemical analysis a standard three electrode system was in place, with 1 mm glassy carbon disc electrode, Ag/AgCl (in 3M KCl) as reference electrode and platinum wire as working electrode. All the potentials are reported Vs Hydroxymethyl Ferrocene (E = +0.385V at SHE) which was added as an internal standard. pH of the solutions used were adjusted using ORION STAR A111 pH Meter (Thermo Scientific) or LMPH-9 (Labman Scientific). Bulk experiments (BE) were done using four-neck glass vessel where three of the necks were occupied by 23 cm coiled Pt electrode as counter electrode, Ag/AgCl (in 3M KCl) as reference electrode, and graphite plastic chip as working electrode, Out of four neck one left was sealed with rubber septum, was used for N_2 purging and for gas collection over headspace (Via gas tight syringe VICI made) with constant stirring. The headspace gas was collected and, analysed using (CIC Dhruva) Gas chromatography (GC) instrument equipped with a TCD detector and 5 A^{o} molecular sieve column for separation of the gases with Argon as carrier. The GC instrument was calibrated using the standard 1% and 2% H_2 gases available.

2. Synthetic Procedure:

The complexes Co(dimethylglyoxime)$_2$Cl$_2$, was synthesised from the previously reported literature.[1] Three different pyridine derivatives such as 3-hydroxy-2-methylpyridine (**L1**), pyridoxamine (**L2**), and pyridoxal phosphate (**L3**) was ligated to Co(dimethylglyoxime)$_2$Cl$_2$ via axial ligation to generate complexes **C1**-**C3**, respectively, according to the following synthetic procedure. 2-methyl pyridine and 4-amino pyridine attached heteroaxial cobaloxime complex has been also synthesized as a control for **C1** and **C2**, respectively.

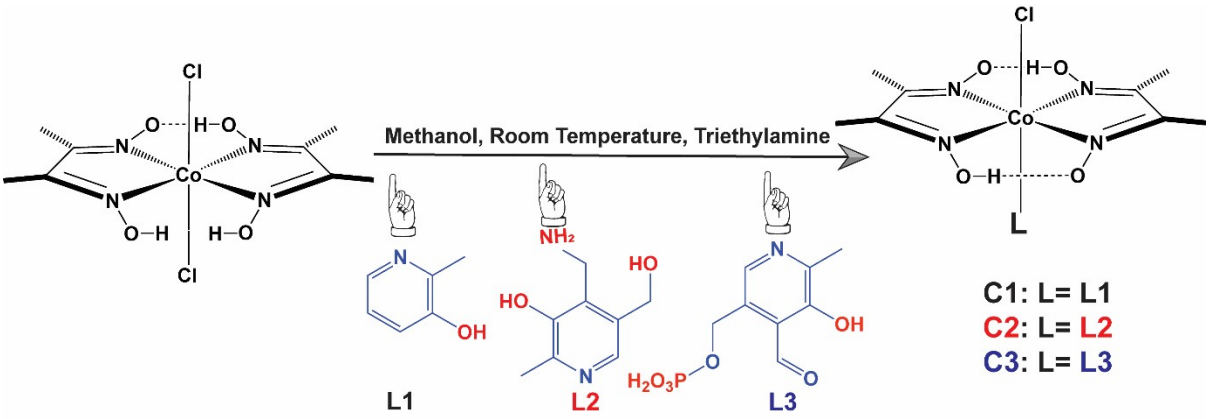

Scheme S1. Scheme for the synthesis of various complexes (**C1**-**C3**).

2.1. Synthesis of C1:

C1 complex was synthesised according to previous reported literature with further modification.[1] 200 mg (0.534 mM) of Co(dmg)$_2$Cl$_2$ was taken in a 50 mL two-neck round bottom flask containing 20 ml of dry methanol. 76 µl (0.534 mM) dry trimethylamine (TEA) was added to the cobaloxime solution with continuous stirring. Then 74 mg (0.534mM) of solid 3-hydroxy-2-methyl pyridine (**L1**) was added to the reaction mixture. Then the reaction mixture was left for stirring under room temperature under an inert (N_2) atmosphere. After 30 minutes a solid yellow product was started to

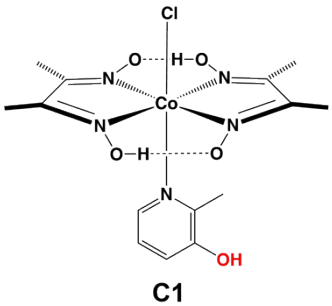

C1

precipitate out. The reaction was further continued for 2 hours until the maximum yield was obtained. The yellow precipitate was collected and washed with cold methanol and dried under vacuum to obtain desired product. Yield= 165 mg (71% wrt. cobaloxime).

UV-Vis in DMF (λ_{max} in nm, ε in parentheses $M^{-1}cm^{-1}$): λ_{max} = 315 (7000), 450 (2100), 550 (750), 700 (200). UV-Vis in Water (λ_{max} in nm, ε in parentheses $M^{-1}cm^{-1}$): λ_{max} = 320 (6900), 430 (2000), 535 (600), 685 (130).

FTIR (in KBr, υ in cm^{-1}): 590 (Co-N pyr), 421 (Co-Cl).

^{1}H NMR (500 MHz, 300K, d^6-DMSO): δ (ppm)= 18.85 (s, 2H, H-bonded oxime); 8.47 (s, 1H, -OH); 7.9 (d, 1H, -Ar); 7.33 (d, 1H, -Ar); 7.12 (m, 1H, -Ar); 2.32 (s, 3H, $-CH_3$); 2.37 (s, 12H, $4CH_3$).

LRMS (ESI, positive mode) m/z^+ for $[M+H]^+$ ion $[C_{14}H_{21}ClCoN_5O_5]$ calculated: 433.06, obtained: 433.16.

2.2. Synthesis of $Co(dmg)_2$-2Me-Py-Cl (control for C1):

The synthesis of the complex by following the similar procedure as mentioned above. In a two-

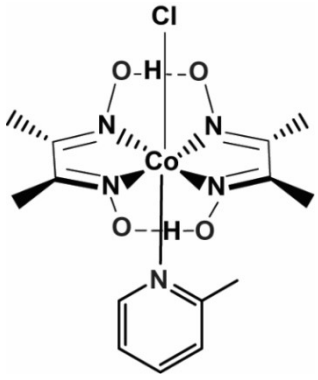

neck round bottom flask, 50 mg of (0.138 mM) of $Co(dmg)_2Cl_2$ was taken with 20 ml dry methanol (purged with nitrogen). 20 µl (0.138 mM) of dry TEA was added to the above solution, followed by 14 µl (0.138 mM) of 2-methyl pyridine, and kept the solution overnight under stirring conditions at room temperature. Then, diethyl ether was added to the reaction mixture and a deep brown solid precipitate was obtained which was further washed with cold methanol and dried under reduced pressure to obtain desired product. Yield= 48 mg (84% wrt. cobaloxime).

^{1}H NMR (400 MHz, 300K, $CDCl_3$): δ(ppm) = 18.42 (s, 2H, H-bonded oxime); 8.46 (d, 1H, -aromatic-ortho-H); 7.54 (dd, 1H, -Aromatic-para-H); 7.12 (dd, 1H, -Aromatic-meta- H,); 7.07 (d, 1H, -Aromatic H); 2.53 (s, 3H, $-CH_3$); 2.15 (s, 12H, $4CH_3$).

LRMS (ESI, positive mode) m/z^{+} for $[M+H+Li]^{+}$ ion $[C_{14}H_{22}ClCoN_5O_4Li]$ calculated: 425.08, obtained: 425.24.

2.3. Synthesis of C2:

The synthesis of complex **C2** was executed analogous to the method described for **C1**. In short,

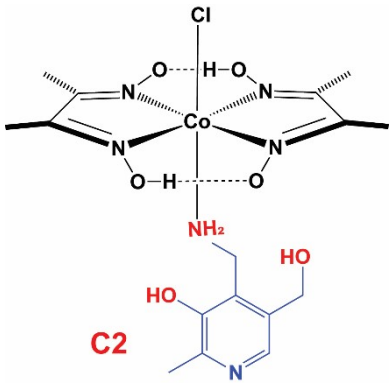

200 mg of (0.534 mM) of $Co(dmg)_2Cl_2$ was taken in a two-neck round bottom flask containing 20 ml dry methanol (purged with nitrogen). 76 µl of dry TEA was added to the cobaloxime followed by 145 mg (0.534 mM) of solid pyridoxamine (**L2**). Then the reaction mixture was continuously stirred and an insoluble yellowish product started to appear after 30 minutes. The reaction mixture was continuously stirred for two hours until the solid precipitate appears. The pure yellowish coloured complex **C2** was obtained following the filtration and subsequent washing with cold methanol. The solid yellow precipitate was further dried under reduced pressure to get the desired product. Yield= 197 mg (75% wrt. cobaloxime).

UV-Vis in DMF (λ_{max} in nm, ε in parentheses $M^{-1}cm^{-1}$): λ_{max} 315 (7500), 370 (2500), 500 (300), 600 (70). UV-Vis in Water (λ_{max} in nm, ε in parentheses $M^{-1}cm^{-1}$): λ_{max} = 325 (7800), 370 (2570), 490 (215), 600 (60).

FTIR (in KBr, υ in cm^{-1}): 647 (Co-NH_2), 420 (Co-Cl).

^{1}H NMR (400 MHz, 300K, d^6-DMSO): δ(ppm) = 18.46 (s, 2H, H-bonded oxime); 8.96 (s, 1H, -aromatic OH); 7.82 (s, 1H, -aromatic OH); 5.34 (s,1H, -OH); 4.25 (2H, Ar-CH_2); 2.89 (4H, broad, NH_2 & Ar-CH_2); 2.51 (s, 12H, 4CH_3) 2.38 (s, 3H, -CH_3).

HRMS (ESI, positive mode) m/z$^+$ for $[M+H]^+$ ion $[C_{16}H_{26}ClCoN_6O_6]$ calculated: 493.1012, obtained: 493.1008.

2.4. Synthesis of Co(dmg)$_2$-4-amino-Py-Cl (control for C2):

The synthesis of control for C2 was carried out by following the method described earlier. In

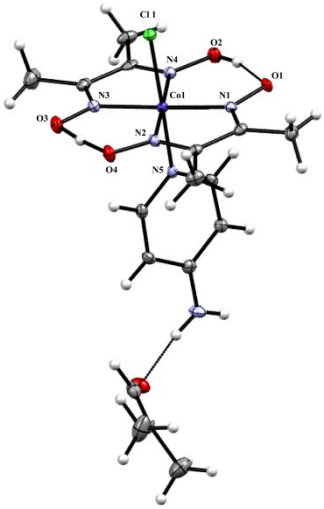

a two-neck round bottom flask, 50 mg of (0.138 mM) of $Co(dmg)_2Cl_2$ was taken with 20 ml dry methanol (purged with nitrogen). 20 µl (0.138 mM) of dry TEA was added to the above solution, followed by 12.98 mg (0.138 mM) of 4-amino pyridine. After 30 minutes an orange precipitate was obtained, washed with cold methanol and dried under reduced pressure to obtain desired product. SC-XRD suitable crystal structure (**CCDC: 2189258**) was obtained from methnol-DMSO mixture by slow evaporation. Yield= 51mg (91% w.r.t. cobaloxime).

^{1}H NMR (400 MHz, 300K, $CDCl_3$): δ(ppm) = 18.56 (s, 2H, H-bonded oxime); 7.41 (d, 2H, -aromatic-ortho-H); 7.26 (dd, 2H, -aromatic-meta-H); 5.39 (s, 2H, -NH_2); 2.30 (s, 12H, 4CH_3).

HRMS (ESI, positive mode) m/z$^+$ for $[M+H]^+$ ion $[C_{13}H_{21}ClCoN_6O_4]$ calculated: 419.0644, obtained: 419.0635.

2.5. Synthesis of C3:

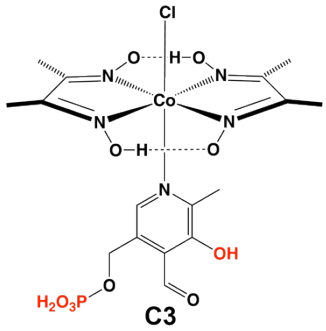

C3

The complex **C3** was synthesised following the similar method for obtaining **C1**-**C2**. Yield= 225.6 mg (74 % wrt. cobaloxime).

UV-Vis in DMF (λ_{max} in nm, ε in parentheses $M^{-1}cm^{-1}$): λ_{max} = 325 (8300), 420 (1450), 550 (147), 670 (50).

UV-Vis in Water (λ_{max} in nm, ε in parentheses $M^{-1}cm^{-1}$): λ_{max} = 315 (7000), 380 (4000), 500 (150), 600 (50).

FTIR (in KBr, ν in cm^{-1}): 594 (Co-N_{pyr}), 428 (Co-Cl).

^{1}H NMR (500 MHz, 300K, d^6-DMSO) δ (ppm) = 18.75 (s, 2H, H-bonded oxime); 10.44 (s, 1H, -CHO); 9.04 (s, 1H, - OH); 8.16 (s, 1H, - Ar); 5.23 (s,2H, -CH_2); 2.63 (s,3H,-CH_3); 2.33 (s, 12H, 4CH_3).

^{31}P: (121.5 MH_z, 300K, d^6-DMSO): δ(ppm) = -1.39 (s. 1P).

HRMS (ESI, positive mode): m/z^+ for (M+H^++Na) ion [$C_{16}H_{24}ClCoN_5O_{10}P$] calculated: 595.0252, obtained: 595.0843.

2.6. Synthesis of unfunctionalized $Co(dmg)_2$Py-Cl:

This complex is already reported in literature. Further to compare your complexes, we prepared

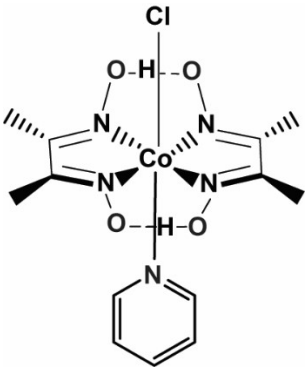

as per previous literature report. 100 mg of $Co(dmg)_2Cl_2$ (0.278 mmol) was taken with 20 ml dry chloroform (purged with nitrogen). 64.75 µl (0.834 mmol) of pyridine was added to the solution and stirred for 20 minutes and the solution turned yellow. 10 ml water was added to the solution mixture and kept 3 hours with vigorous stirring condition. The chloroform layer was extracted, washed with hot acetone and dried under reduced pressure to obtain desired product. Yield= 97 mg (87% wrt. cobaloxime).

^{1}H NMR (400 MHz, 300K, $CDCl_3$): δ(ppm) = 18.16 (s, 2H, H-bonded oxime); 8.30 (d, 2H, -Aromatic-ortho-H); 7.72 (dd, 2H, -Aromatic-para-H); 7.25 (d, 2H, -Aromatic-meta-H); 2.42 (s, 12H, $4CH_3$).

HRMS (ESI, positive mode) m/z$^+$ for $[M+H]^+$ ion $[C_{13}H_{20}ClCoN_5O_4]$ calculated: 404.0535, obtained: 404.0530.

3. Electrochemical Evaluation:

The electro chemical behavior of the three catalysts (**C1**-**C3** and control complexes) was analyzed using cyclic voltammetry technique, all the complexes were studied in aqueous medium, 0.1 M MES buffer was used for preparing the pH solution required for analysis (pH 7.0 to 4.0), besides the supporting electrolyte 0.1M Na_2SO_4 was used. CVs were performed using 1mm glassy carbon disc working electrode, Ag/AgCl (in 3M KCl) as reference electrode, Pt-wire as counter electrode. All the potentials are reported here against standard hydrogen electrode (SHE). Concentrations of the solutions were kept 0.5 mM for all the cyclic voltammetry studies, unless stated otherwise. Studies were carried out using 5 ml capacity glass cell, covered with PTFE cap with four openings, and three were used for electrodes and the remaining one for the argon gas purging. The bulk electrolysis was performed in four neck glass vessel of 170 ml capacity, the three openings were used by three electrodes and the fourth one was used for nitrogen purging and gas collection. Plastic chip with the active area dimensions of 2.3 cm × 2 cm was used as working electrode, Ag/AgCl in 3M

4. Calculation of Faradaic Efficiency (FE) and TON for HER catalysis: KCl as reference electrode, coiled platinum wire as counter electrode.

Both faradic efficiency (FE) and turn over number (TON) have been calculated as per following literature with slight modification.[2]

4.1. FE calculation for C1 during electro-catalytic HER at pH 7.0:

After 1-hour, overall charge passed through bulk electrolysis = (5.5-0.5)C = 5C [blank solution charge = 0.5C]

2×96485C charge passed during HER is equivalent to 22400 ml of H_2

5C charge passed during HER is equivalent to $\frac{22400 \times 5}{2 \times 96485} = 0.580\ ml$ H_2

Through GC experiment, amount of H_2 detected through headspace $= 0.481\ ml$ (calibrated by control)

So, Faradic Efficiency (FE) = $\frac{0.481}{0.580} \times 100 = 83\ \%$

The amount of H_2 produced during HER catalysis $= \frac{0.481}{22.4} = 0.0214\ mmol$

Catalyst concentration in mmol $= 15 \times 0.02 = 0.3\ \mu M$

TON $= \frac{0.0214\ mM}{0.3\ \mu M} = 72$

4.2. Foot-of-the Wave Analysis (FOWA): Ideal catalytic activity during electrocatalysis can be accurately determined by the foot-of-the-wave analysis. It has been developed by Savéant and coworkers[3] ***Equation S1*** represents the current (i) for an EECC and ECEC process.[4]

$$i = \frac{2FAC_{P^0}\sqrt{Dk_{obs}}}{1 + exp\{\frac{F}{RT}(E - E_{cat/2})\}} \quad (Equation\ S1)$$

i = catalytic current. F = Faraday's constant. A = surface area of the electrode. C_{P^0} = bulk concentration of the catalyst. D=diffusion coefficient. k_{obs} = rate constant of the catalyst. The Randle-Sevick equation (***Equation S2***) is used to determine the peak current for a homogeneous, diffusion-controlled process.[5]

$$i_p = 0.4463FAC_{P^0}\sqrt{\frac{F\nu D}{RT}}\ (Equation\ S2)$$

Dividing ***Equation S1*** by ***Equation S2*** *yields* ***Equation S3***.

$$\frac{i}{i_p} = \frac{2\sqrt{\frac{RT}{Fv}}\sqrt{k_{obs}}}{0.4463} \times \frac{1}{1 + exp\{\frac{F}{RT}(E - E_{cat/2})\}} \quad (Equation\ S3)$$

The plot of $\frac{i}{i_p}$ vs. $\frac{1}{1 + exp\{\frac{F}{RT}(E - E_{cat/2})\}}$ provides the slope (m) and from it k_{obs} (**Figure S3**) is calculated.[6]

$$m = \frac{2\sqrt{\frac{RT}{Fv}}\sqrt{k_{obs}}}{0.4463} (Equation\ S4)$$

$$k_{obs} = \frac{m^2(0.4463)^2 Fv}{4RT} (Equation\ S5)$$

From the above equation kinetic rate of the catalyst will be calculated.

4.3. Rate calculation (k_{obs}) of C2 catalyst at pH 7 from FOWA (*Figure S3A*):

$v =$ scan rate = 1 V/s. $m =$ slope = 24.93

$$k_{obs} = \frac{24.93^2 \times (0.4463)^2 \times 96485\frac{C}{mol} \times 1\frac{V}{s}}{4 \times 8.314\frac{J}{mol.K} \times 298\ K}$$

$$k_{obs} = 1202\ s^{-1}$$

5. Photocatalytic H_2 Production: Photocatalytic H_2 Production studies were carried out at in aqueous buffer medium in a Schlenk flask of capacity 53 ml. 5×10^{-3} M Eosin-Y stock solution was prepared as photosensitizer and from that solution the required conc. was prepared by dilution. Similarly, 1×10^{-3} M freshly prepared catalyst concentration was prepared and from it the required concentration was prepared for the experiment (Final concentration of the solution is: 50×10^{-6} M Eosin-Y (PS) and 25×10^{-6} M). All the experiments were performed at pH 7 using

0.1M (MES) buffer unless stated otherwise. Total volume of reaction mixture was 20ml, 10% TEOA was used as sacrificial electron donor (SED). The photocatalytic experiments were carried out using (SLS301) Thor lab instrument with wavelength range from 350-2700 nm, with additional band pass filter 350-610 nm was used to filter only the visible portion of light required by Eosin-Y PS. The laser power was fixed at 40 mW/cm^2 and the beam size was fixed at 3.80 cm^2 for all the experiments. Before each experiment the sample was purged with argon gas for 30 min to degas amount of O_2 present. During the experiment, 0.5 ml of headspace gas was collected and injected into the GC instrument via VICI made Leur-lock gas tight syringe over period of time.

6. Single Crystal X-ray Diffraction study:

Crystals of **C2** complex was grown by solvent diffusion method from methanol/diethyl ether and control for C2 from methanol-DMF solvent. Suitable crystal was selected and mounted on a cryo-loop using cryoprotectant paraffin oil. Single crystal diffraction data were collected at 100(1) K on a Bruker D8 Quest diffractometer equipped with an Incoatec Microfocus Source (IμS 3.0 Mo Kα, λ = 0.71073 Å) and a PHOTON II CCD detector. X-ray diffraction intensities were collected, integrated and scaled with APEX4 software. Empirical absorption correction was applied to the data by employing multi-scan method with SADABS programming.[7] Structure was solved by intrinsic phasing with SHELXT and refined by full-matrix least-square methods on F^2 using SHELXL, using the ShelXle interface.[8] All non-hydrogen atoms were refined with anisotropic displacement parameters. The hydrogen atoms were introduced at a calculated positions and were treated as riding atoms with an isotropic displacement parameter, C-H = 0.93-0.98 A° with Uiso(H) = 1.5 Ueq(C) for methyl groups, Uiso(H) = 1.2 Ueq(C, N) for all other C-H and N-H bonds and O-H = 0.82 A˚ [Uiso (H) = 1.5 Ueq(O)]. The molecular plot was drawn with Mercury 4.2.[9] Crystal data, data collection and structure refinement details are summarized in **Table S4. C2** complex crystalizes with an unreacted cobaloximes to

maintain overall charge neutral. The crystallographic information of **C2** co-crystals (CCDC 2152879) and control for **C2**: 4-amino pyridine cobaloxime (CCDC **2189258)** can be obtained free of charge from the Cambridge Crystallographic Data Centre via www.ccdc.cam.ac.uk

7. Supplementary Figures:

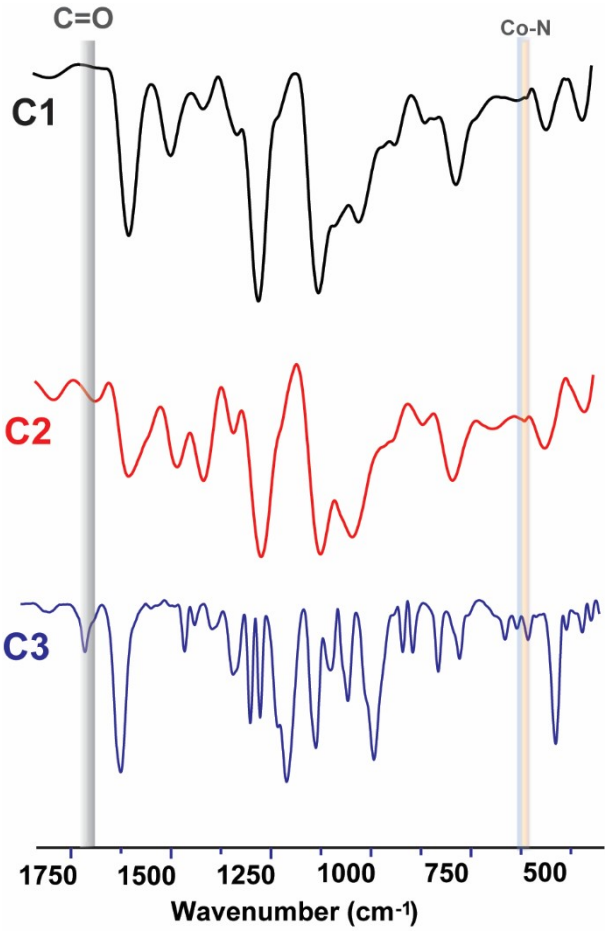

Figure S1: FTIR data for the solid complexes (**C1-C3**). Data were recorded at room temperature by preparing KBr pellet scanning from 386-4000 cm^{-1}.

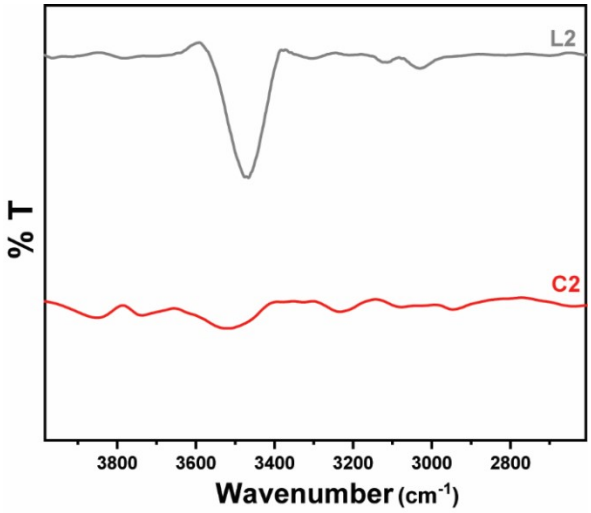

Figure S2: FTIR spectrum comparison beween **L2** (grey trace) and **C2** (red trace). 2600-4000 cm^{-1} region is heighligted. Data were recorded by preparing KBr pellet and recorded at room temperature.

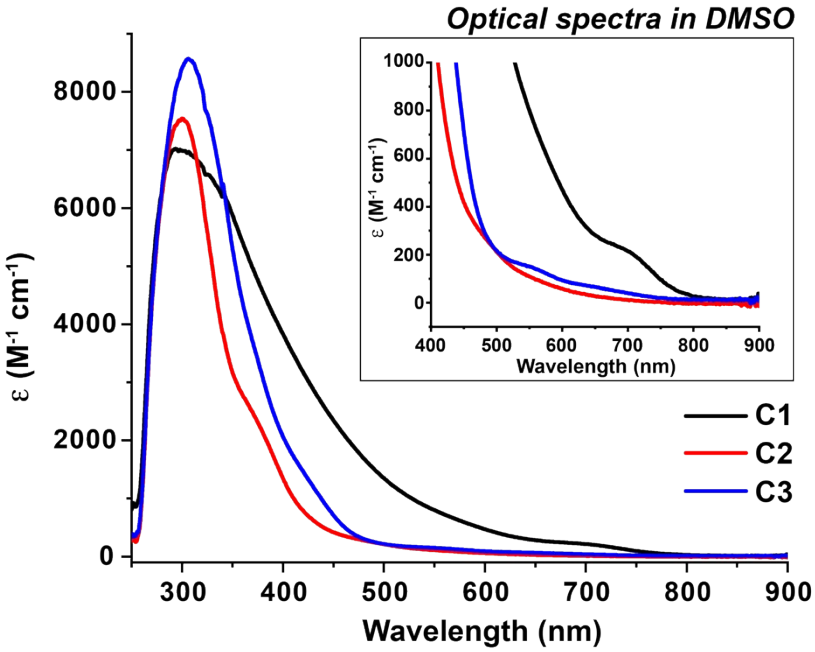

Figure S3. UV-Vis spectrum for the complexes (**C1**: black trace; **C2**: red trace; **C3**: blue trace) recorded in dimethyl sulfoxide (DMSO) solvent. Inset figure depicts the d-d transition for the complexes. Data were recorded at room temperature.

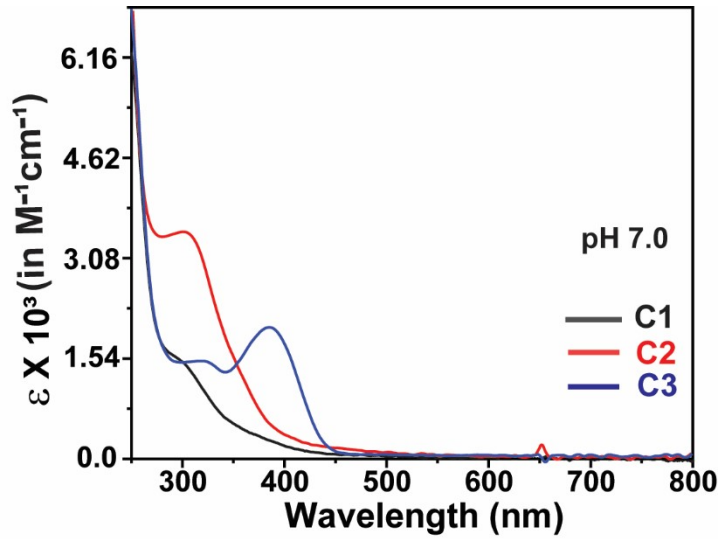

Figure S4. UV-vis spectrum for the complexes (**C1**: black trace; **C2**: red trace; **C3**: blue trace) recorded in pH 7.0 aqueous MES buffer. Data were recorded at room temperature.

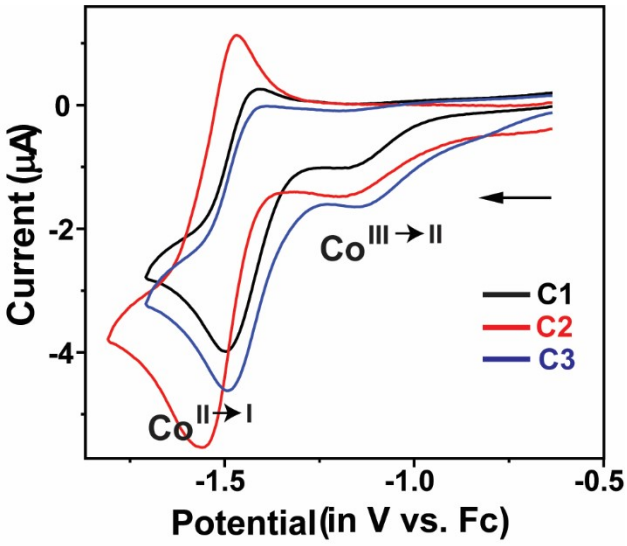

Figure S5: Comparative cyclic voltammetry(CV) data recored for 1 mM complexes **C1** (black trace); **C2** (red trace); **C3** (blue trace). Data was recored at room termperature under N_2 pressure. Insert arrow depics origin and scan sweep direction.

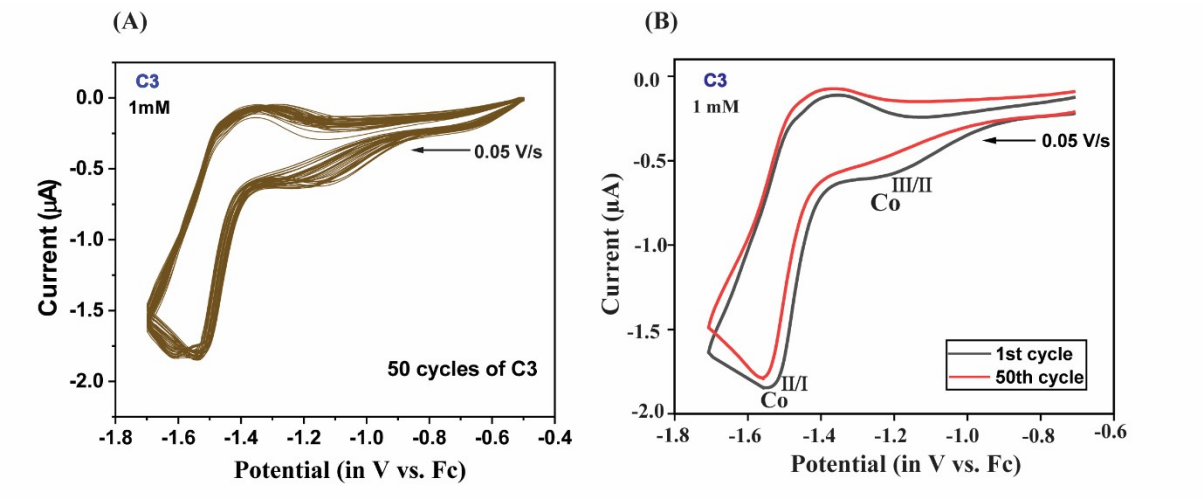

Figure S6: (A) Multiple cycle CV data for 1 mM **C3** complex recorded in MeCN solvent. (B) 1st and 50th cycle CV data has been compared. All the data were recorded at 0.05 V/s scan rate. Black CV data is for 1st cycle and Red one is for 50th cycle.

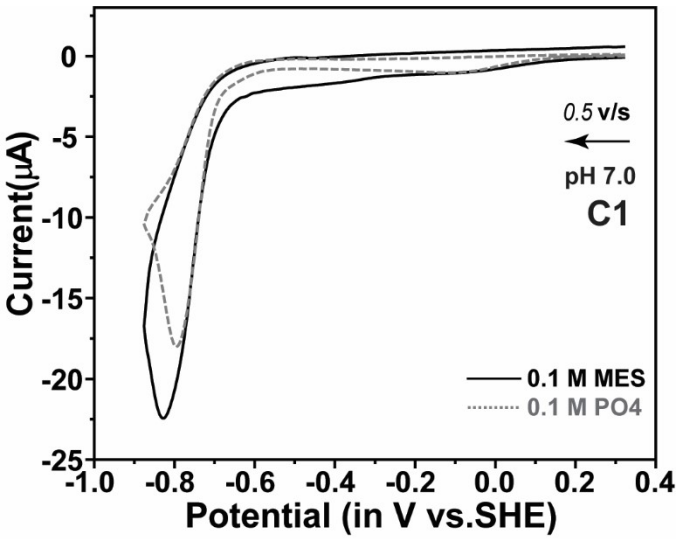

Figure S7: Comparative cyclic voltammetry recorded for 0.5 mM **C1** complex recorded at 0.1 M pH 7.0 MES buffer (solid black trace); and at 0.1 M pH 7.0 phosphate buffer (dotted grey trace). Data were recorded at room temperature at 0.5 v/s scan rate. Inset arrow depicts origin and scan direction.

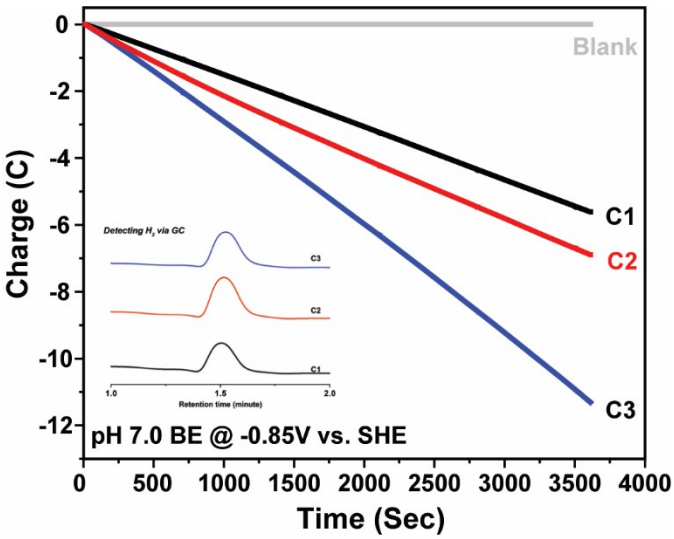

Figure S8. Bulk electrolysis charge passed data recorded for the 0.025 mM complexes **C1-C3**. Data were recorded at aqueous pH 7.0 buffer applying potential of -0.85 V vs. SHE. Inset figure represents GC data after injecting 0.5 ml headspace sample during BE.

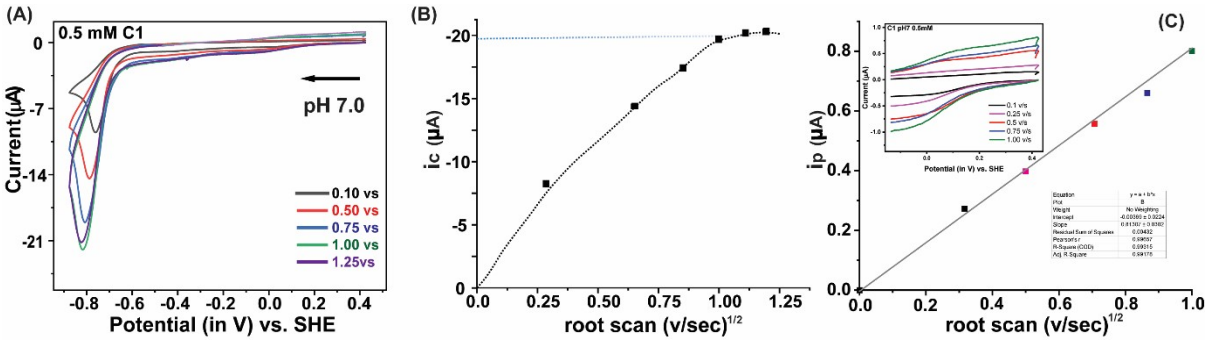

Figure S9: (A) Comparative cyclic voltammogram data for 0.5 mM **C1** at different scan rate. (B) i_c and (C) i_p is plotted against root scan rate. Data were recorded at pH 7.0 under anaerobic conditions. All data were recorded at 1 Vs^{-1} scan rate. The horizontal arrow depicts the origin and scan direction.

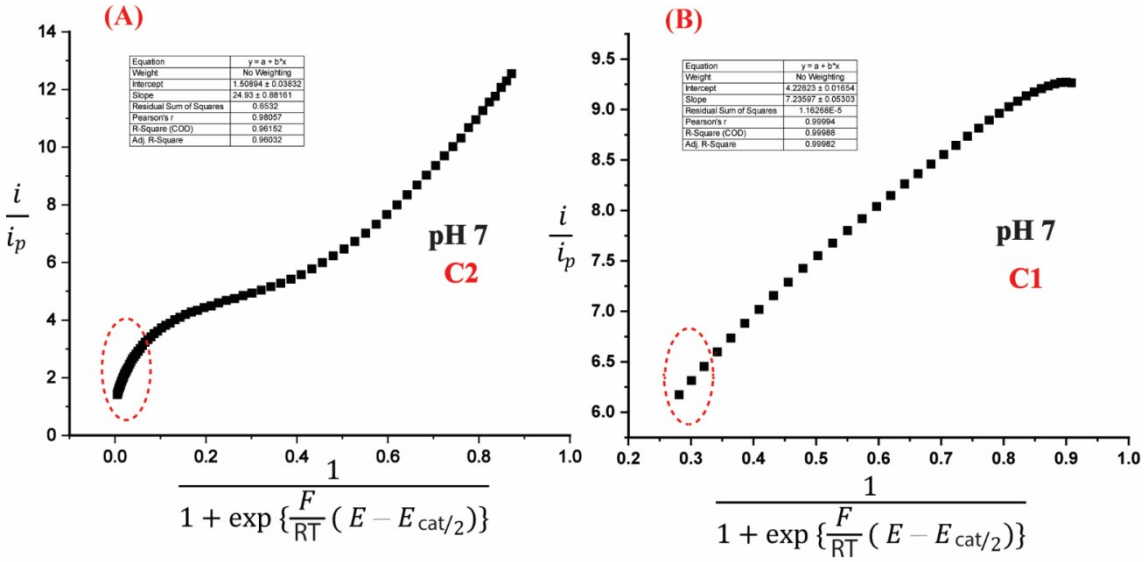

Figure S10: Foot of the wave analysis (FOWA) of (A) **C2** and (B) **C1**at pH 7 under N_2 in neutral pH solution. Here $\frac{i}{i_p}$ is plotted against $\left[\frac{1}{1+exp\{\frac{F}{RT}(E-E_{cat/2})\}}\right]$. The red dotted lines demonstrates the measured wave section taken for FOWA.

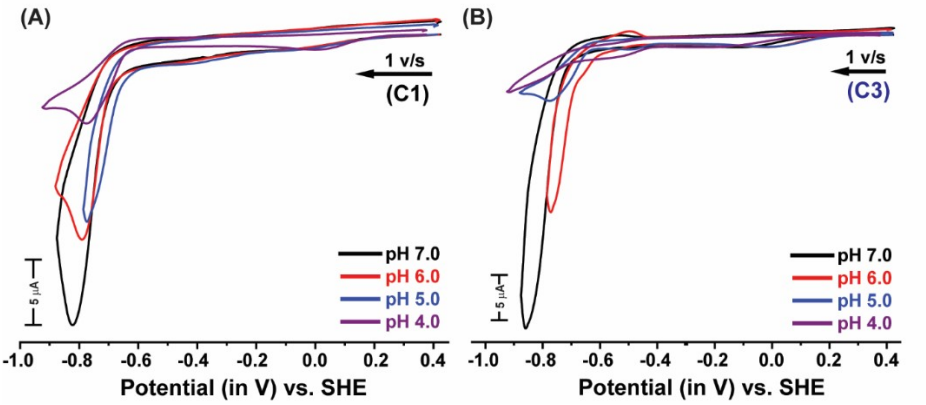

Figure S11. Comparative cyclic voltammogram data at different pH: (A) for complex **C1** (B) for complex **C3**. Data were recorded at pH 7.0 to pH 4.0 (pH 7.0: black trace; pH 6.0: red trace; pH 5.0: blue trace; pH 4.0: violet trace) under anaerobic conditions. All data were recorded at 1 Vs^{-1} scan rate at room using 0.5mM of each complex. The horizontal arrow depicts the initial scan direction.

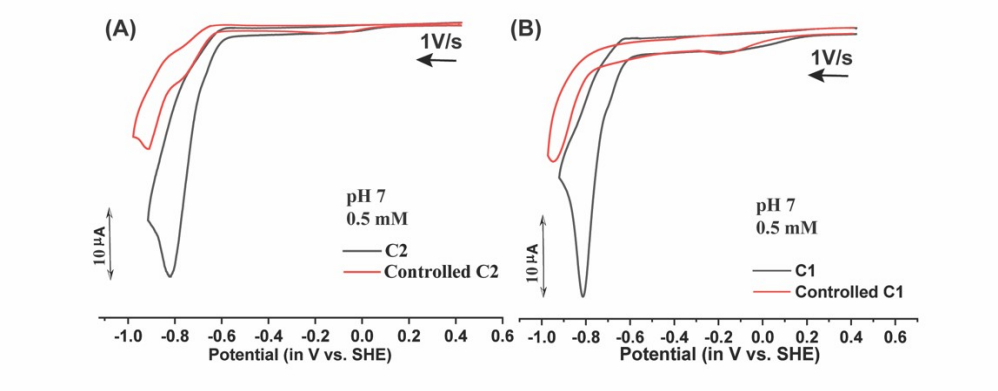

Figure S12. Comparative CV data for 0.5 mM complexes (black trace), (A) **C2** complex and (B) **C1** complex, with their controlled one (red traces). All the data were recorded at 0.1M MES buffer (pH-7.0) at room temperature. Inside arrow indicates origin and direction of scan.

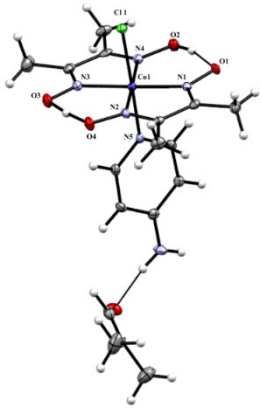

Figure S13. The crystal structure of cobaloxime-4-aminopyrdine chloride complex. Color codes for the crystal structure Co: violet; N: blue, C: pink, O: red; Cl: green.

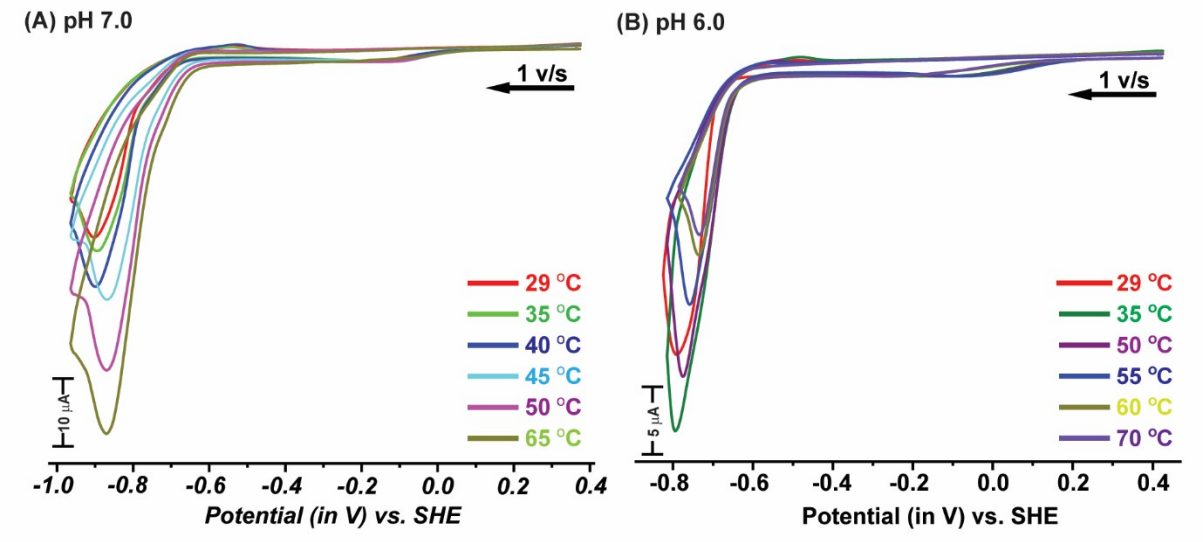

Figure S14. Comparative cyclic voltammogram data for 0.5 mM **C2** at (A) pH 7.0; (B) pH 6.0 in different temperature condition under anaerobic conditions. All data were recorded at 1 Vs^{-1} scan rate at room temperature. The horizontal arrow depicts the initial scan direction.

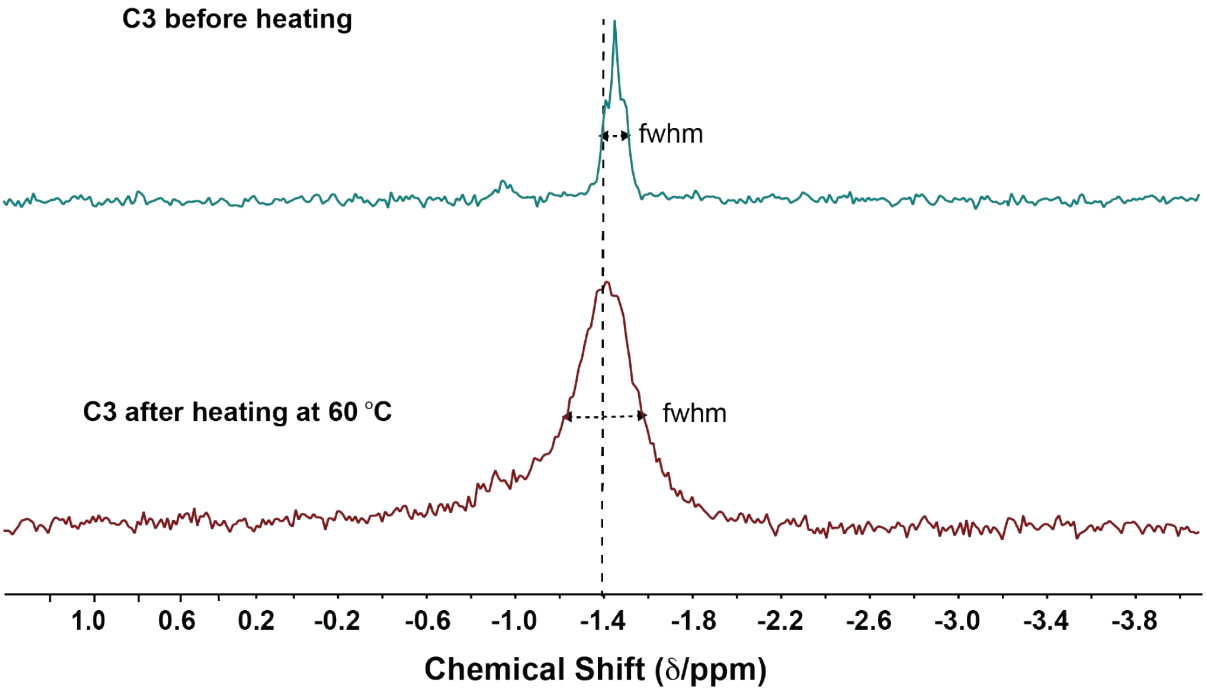

Figure S15. The comparative $^{31}P\{^{1}H\}$ NMR spectra recorded for complex **C3** before (cyan trace) and after heating at 60 °C (brown trace) for 20 minutes. All the data are recorded at room temperature containing in a solution of d^6-DMSO containing 30% D_2O.

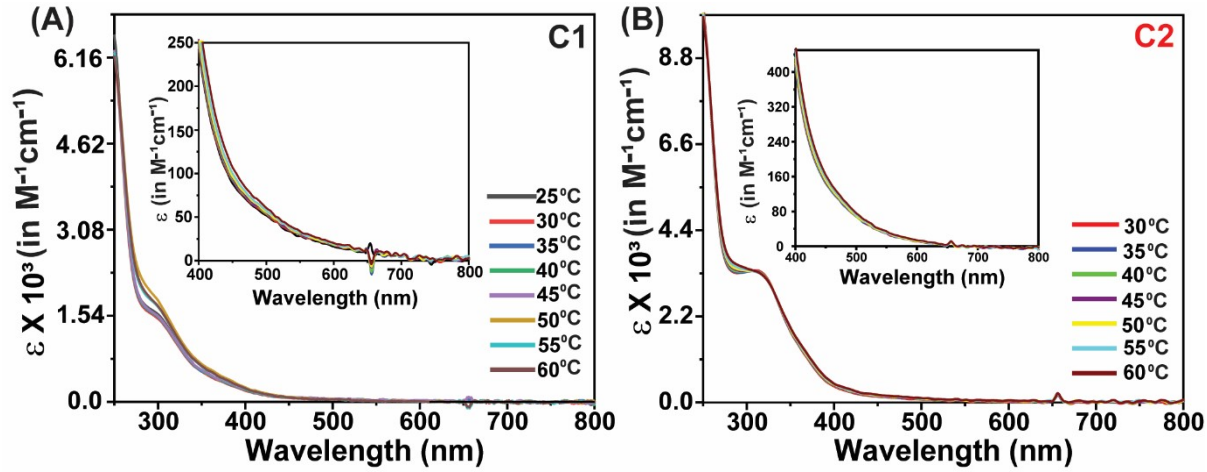

Figure S16. Comparative UV-vis spectrum for the (A) complex **C1** and (B) complex **C2**; at variable temperature conditions. Inset figure depicted the enlarge portion of 400-800 nm range. Data was recorded at pH 7.0 using 0.1M MES aqueous buffer.

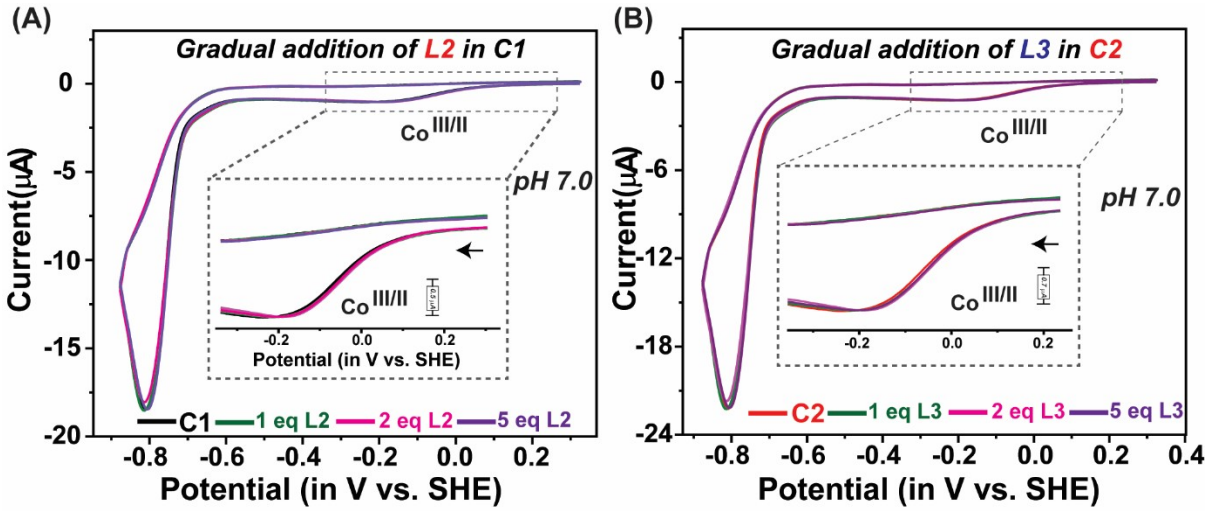

Figure S17. The cyclic voltammograms recorded for (A) **C1** (black trace), (B) **C2** (red trace) after adding 1eq (green trace); 2eq (pink trace); 5eq (purple trace) corresponding hetero ligands. Data were recorded under Argon atmosphere at pH 7.0 aqueous 0.1 buffer solution. 1 mm glassy carbon disc, a Pt wire, and Ag/AgCl (in 3M KCl) was used as working, counter, and reference electrode respectively. The horizontal arrow indicates the initial scan direction.

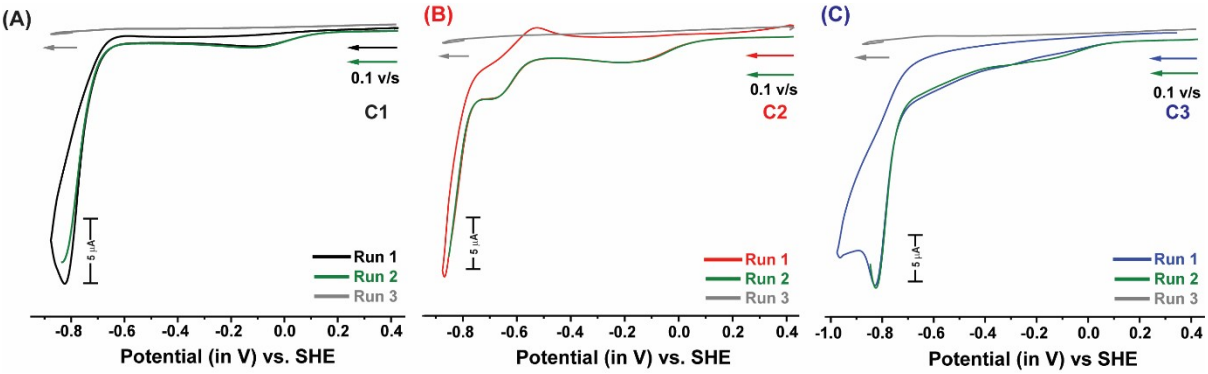

Figure S18. Rinse test of complexes (A) **C1**, (B) **C2**, (C) **C3**, at pH 7.0. Run 1 is a complete run recorded for complexes. The electrode was polished and cleaned after Run 1. Run 2 (green trace) was a scan of the same complex in same solution only cathodic scan up to -0.85 V vs SHE was recorded. Electrode was only rinsed with water without any polishing and used for Run 3 (grey trace). Run 3 was done in different pH 7.0 buffer solution which does not contains any complex. Run 3 scan was started from -0.83 V vs. SHE. No significant reduction current was observed in the third run around -0.85 V vs. SHE to -0.45V vs. SHE, which excludes possibility of heterogeneous species formation during cathodic scan was beyond -0.80 V vs. SHE. Data was recorded at room temperature. Solid arrow indicates origin and direction of each scan.

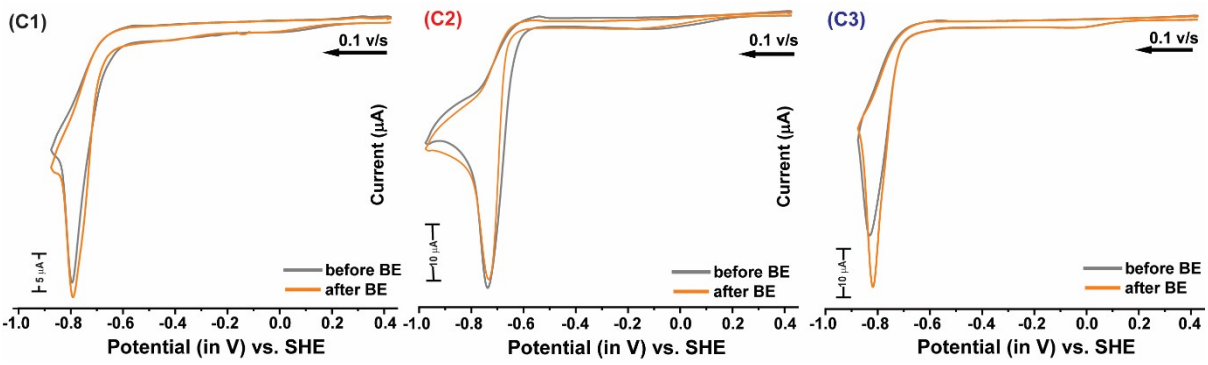

Figure S19. The comparative data from cyclic voltammetry (0.1 V/s scan rate) for complexes **C1**-**C3** sample pre- (grey trace) and post-bulk electrolysis samples (orange trace). The bulk electrolysis was performed at -0.85 V vs. SHE for 60 minutes.

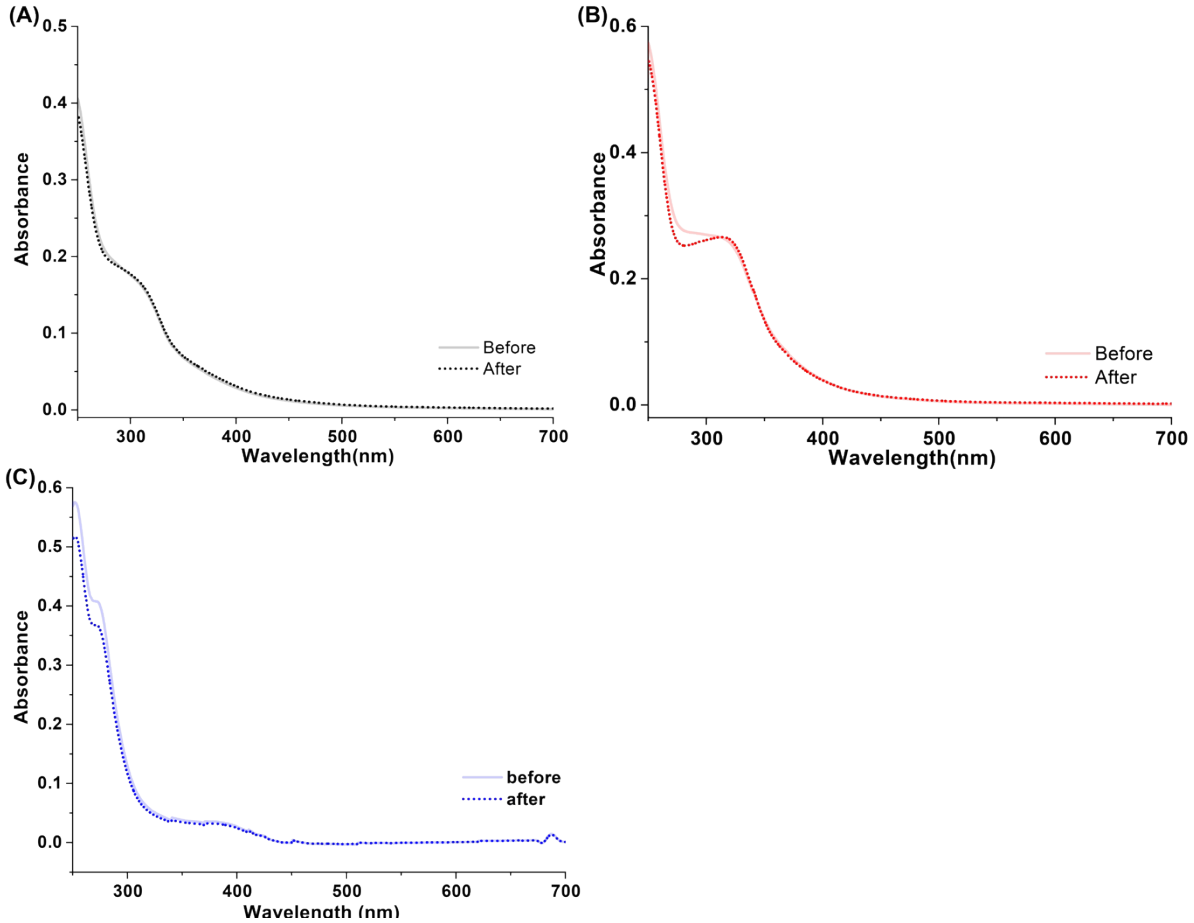

Figure S20. The comparative data from optical spectroscopy for complexes (A) **C1**, (B) **C2** and, (C) **C3** sample pre- (solid trace) and post-bulk electrolysis samples (dotted trace). The bulk electrolysis was performed at -0.85 V vs. SHE for 60 minutes.

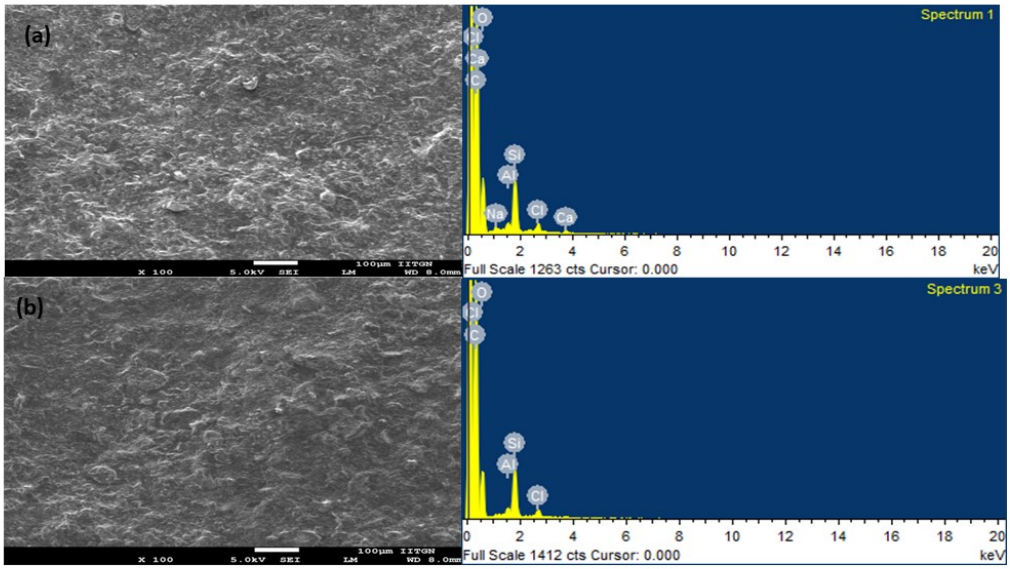

Figure S21. SEM and EDS analysis of graphite chip working electrode before and after bulk experiment. (a) (SEM image analysis and EDS analysis) Bulk electrolysis before catalysis, was recorded at -0.85 V vs SHE of **C2** complex at pH-7.0 for 3600 secs using Ag/AgCl reference electrode Pt coil as counter electrode and graphite chip as working electrode [generated from graphite powder and poly(methyl methacrylate)]. (b) (SEM image analysis and EDS analysis) after Bulk electrolysis of **C2** complex using plastic chip working electrode, no trace of cobalt was found onto the working electrode.

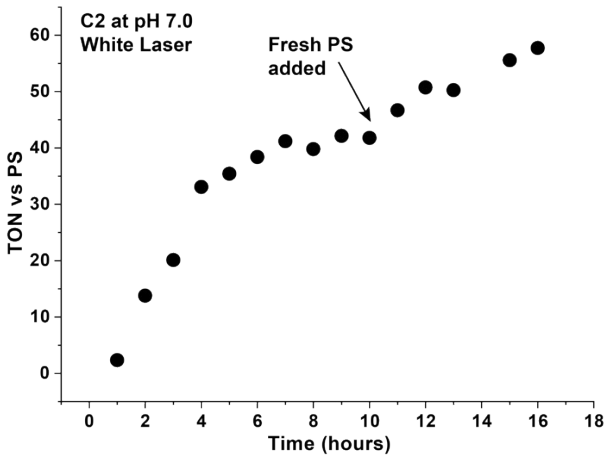

Figure S22. Observed TOF during photocatalytic experiments for **C2**, recorded at pH 7.0 using Eosin-Y as PS.

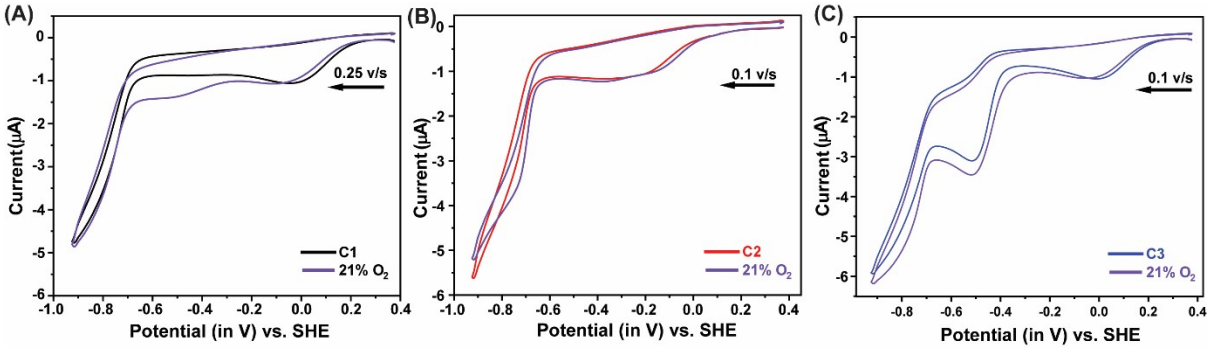

Figure S23. The cyclic voltammograms recorded for (A) **C1**, (B) **C2** and (C) **C3** complexes under air (purple trace) and under Argon atmosphere at pH 7.0 aqueous solution. 1 mm glassy carbon disc, a Pt wire, and Ag/AgCl (in 3M KCl) was used as working, counter, and reference electrode respectively. The horizontal arrow indicates the initial scan direction.

8. Supplementary Tables:

Table S1. Optical spectral features[a] observed for **C1**-**C3** and their corresponding assignments

Complex	Solvent	π-π* transition λ_{max}/nm (ε/$M^{-1}cm^{-1}$)	LMCT transition λ_{max}/nm (ε/$M^{-1}cm^{-1}$)	*d-d* transition λ_{max}/nm (ε/$M^{-1}cm^{-1}$)
C1	DMSO	315 (7000)	450 (2100)	550 (750), 700 (200)
	pH 7.0	255 (7232)	305 (1532)	535 (130), 685 (90)
C2	DMSO	315 (7500)	370 (2500)	500 (300), 600 (70)
	pH 7.0	250 (7300)	340 (4235), 320 (3900)	490 (105), 600 (60)
C3	DMSO	325 (8300)	420 (1450)	550 (147), 670 (50)
	pH 7.0	255 (7180)	380 (4000), 310 (1530)	500 (150), 600 (50)

[a]All data recorded at room temperature.

Table S2. Electrocatalytic H_2 production reactivity (Turnover frequency/TOF[a]; overpotential requirement/OP, and turnover number/TON)[b] by complexes **C1-C3** in aqueous solution. Rate calculated form i_{cat}/i_p ratio (Equation 2).

Complex	Electrocatalytic							
	pH 7.0		pH 6.0		pH 5.0		pH 4.0	
	TOF (s^{-1})	OP (mV)	TOF (s^{-1})	OP (mV)	TOF (s^{-1})	OP (mV)	TOF (s^{-1})	OP (mV)
C1	621 (±45)	338 (±10)	383 (±20)	324 (±10)	229 (±20)	410 (±10)	52 (±5)	455 (±10)
C2	864 (±50)	385 (±10)	705 (±20)	433 (±10)	313 (±20)	375 (±10)	20 (±10)	523 (±10)
C3	1125 (±50)	373 (±10)	338 (±20)	363 (±10)	39 (±10)	400 (±10)	12 (±10)	550 (±10)

[a]All the TOFs are calculated at 1.0 Vs^{-1}.
[b]The error range is calculated from three independent runs for each sample.
[c]PS: photosensitizer.

Table S3. Comparison table for the cobalt complexes reported for homogeneous electrocatalytic HER from aqueous buffer medium.

Name of the Complex		Electrocatalytic HER from aqueous medium				Ref
		Working Medium	TOF (s^{-1})	OP (mV)	TON	
1.	Co-salen tyrosine	pH 2.0	190	775	-	[10]
2.	$Co(DmgBF_2)_2(CH_3CN)_2$	pH 2.2	-	442	5×10^5 (7h)	[11]
3.	Co(Iminopyridine)	pH 4-9	2.5 h^{-1}	-	-	[12]
4.	$[(RPY_5Me_2)\ Co(L)]^{2+}$ R= H, CF_3, NMe_2	pH 7	0.3 (12h)	887	5.5×10^4 (60h)	[13]
5.	$[Co(CR)(OH_2)_2]\ (ClO_4)_3$	pH 2.2	-	500	12 (2h)	[14]

6.	[(DPABpy)Co(H_2O)](PF_6)$_3$	pH 7	0.08 (1h)	987	300 (1h)	[15]
7.	[Co(DO)(DOH)Pn(OH_2)$_2$](ClO_4)$_2$	pH 2.2	-	500	23 (2h)	[16]
8.	[(btzPx)CoL] (BF4)2	pH 7	0.14 (60h)	837	1.6x 10^5 (60h)	[17]
9.	[(15Pydiene N_5)Co]$^{2+}$	pH 7	2210	680	-	[18]
10	CoMC6*a	pH 6.5	-	680	2.3x10^5 (3h)	[19]
11	Ht-CoM61A	pH 7	-	830	1.1 x10^5 (6h)	[20]
12.	CoGGH	pH 8	-	600	310 (2.5h)	[21]
13.	[CoP][Et_3N]	pH 7	-	287	-	[22]
14.	CoMP11-Ac	pH 7	-	852	2.5x10^4 (4h)	[23]
15.	His_Co	pH 7	4525	477	-	[24]
16.	Co_Tyrosine	pH 7	8830	507	-	[25]
17.	Co(bpy)$_2$(SCN)$_2$	pH 7	699.6 h-1	837.6	-	[26]
18.	**C1**	pH 7, 60 ^oC	961	304	-	**This Work**
19.	**C2**	pH 7, 60 ^oC	3635	321	-	**This work**
20.	**C3**	pH 7, 35 ^oC	1925	375	-	**This work**

Table S4. The redox potential and Faradaic efficiency (FE) calculation from bulk electrolysis (at pH 7.0) for complexes **C1**-**C3**.

Complex	In CH_3CN (V vs. Fc)		$E_{Co(III/II)}$ (V vs. SHE)				Faradaic efficiency (FE) recorded at pH 7.0 (%)
	¥Co (III/II)	£Co (II/I)	pH 7.0	pH 6.0	pH 5.0	pH 4.0	
C1	-1.17	-1.45	-0.03	-0.02	-0.02	-0.01	83 (±5)
C2	-1.18	-1.51	-0.13	-0.16	-0.18	-0.28	91 (±4)
C3	-1.14	-1.44	-0.08	-0.01	-0.01	-0.04	87 (±5)

¥: peak position; £: half catalytic position.

Table S5. Crystal data and refinement details of compound **C2** and control for **C2** (4-amino pyridine cobaloxime).

Identification code	**C2.Cobaloxime.H_2O**	**4-amino pyridine Cobaloxime. DMF**
Empirical formula	$C_{24}H_{43}Cl_3Co_2N_{10}O_{11}$	$C_{17}H_{27}ClCoN_6O_5$
Formula weight	871.89	489.82
Temperature/K	108(2)	100(2)
Colour	yellow	yellow
Crystal system	Monoclinic	Monoclinic
Space group	$P2_1/n$	$P2_1/n$
a/Å	8.3675 (3)	8.1412(2)
b/Å	18.8072 (5)	11.7627(3)
c/Å	22.1321 (7)	22.2100(6)
α/°	90	90
β/°	91.744 (3)	94.958(10)
γ/°	90	90
Volume/Å^3	3481.30 (19)	2118.93(9)

Z	4	4
ρ_{calc}g/cm^3	1.664	1.535
μ/mm^{-1}	1.254	0.978
F(000)	1800.00	1020.00
Crystal size/mm^3	0.156 × 0.121 × 0.056	0.165 x 0.121 x 0.056
Radiation	MoKα (λ = 0.71073)	MoKα (λ = 0.71073)
Data Collection		
2Θ range for data collection/°	3.682 to 49.998	3.93 to 49.994
Index ranges	-9 ≤ h ≤ 9, -22 ≤ k ≤ 22, -26 ≤ l ≤ 26	-8 ≤ h ≤ 9, -23 ≤ k ≤ 26, -13 ≤ l ≤ 13
Reflections collected	63643	11573
Independent reflections	6113 [R_{int} = 0.1087, R_{sigma} = 0.0570]	3717 [R_{int} = 0.0475, R_{sigma} = 0.0506]
Data/restraints/parameters	6113/0/478	3717/0/287
Goodness-of-fit on F^2	1.044	1.033
Final R indexes [I>=2σ (I)]	R_1 = 0.0394, wR_2 = 0.0803	R_1 = 0.0383, wR_2 = 0.0874
Final R indexes [all data]	R_1 = 0.0580, wR_2 = 0.0879	R_1 = 0.0501, wR_2 = 0.0939
Largest diff. peak/hole / e Å^{-3}	0.32/-0.40	0.71/-0.37
CCDC	***2152879***	***2189258***

Table S6. Table for TOF and OP data calculated from CV data recorded at pH 7.0 with varying temperature (29 °C to 70 °C) for complexes **C1**-**C3**.

Temp (°C)	C1		C2		C3	
	ΨTOF (S^{-1})	OP (mV)	TOF (S^{-1})	OP (mV)	TOF (S^{-1})	OP (mV)
29	621 (±45)	337 (±10)	864 (±40)	385 (±10)	1125 (±40)	373 (±10)
35	641 (±40)	338 (±10)	930 (±40)	371 (±10)	1925 (±40)	372 (±10)
40	635 (±40)	316 (±10)	974 (±50)	351 (±10)	-nr-	-nr-
45	-nr-	-nr-	1362 (±50)	345 (±10)	-nr-	-nr-
50	786 (±50)	306 (±10)	1518 (±45)	321 (±10)	1362 (±55)	358 (±10)
55	-nr-	-nr-	2542 (±40)	321 (±10)	808 (±50)	358 (±10)
60	961 (±50)	304 (±10)	3635 (±55)	321 (±10)	540 (±40)	358 (±10)
70	-nr-	-nr-	-nr-	-nr-	373 (±45)	355 (±10)

*nr: Data not recorded, Ψ: TOF reported by using i_{cat}/i_p ratio (Equation 2).

References:

1 G. Schrauzer, G. W. Parshall and E. R. Wonchoba, *Inorg. Synth.*, 1968, **11**, 61–70.

2 A. Ali, D. Prakash, P. Majumder, S. Ghosh and A. Dutta, *ACS Catal.*, 2021, **11**, 5934–5941.

3 C. Costentin, S. Drouet, M. Robert and J.-M. Savéant, *J. Am. Chem. Soc.*, 2012, **134**, 11235–11242.

4 V. C.-C. Wang and B. A. Johnson, *ACS Catal.*, 2019, **9**, 7109–7123.

5 E. S. Rountree, B. D. McCarthy, T. T. Eisenhart and J. L. Dempsey, *Inorg. Chem.*, 2014, **53**, 9983–10002.

6 R. J. DiRisio, J. E. Armstrong, M. A. Frank, W. R. Lake and W. R. McNamara, *Dalton Trans.*, 2017, **46**, 10418–10425.

7 G. M. Sheldrick, *Univ. Gött. Gött. Ger.*

8 G. M. Sheldrick, *Acta Crystallogr Sect Found Crystallogr A*, 2008, **64**, 112–122.

9 C. F. Macrae, P. R. Edgington, P. McCabe, E. Pidcock, G. P. Shields, R. Taylor, M. Towler and J. V. D. Streek, *J. Appl. Crystallogr.*, 2006, **39**, 453–457.

10 S. Khandelwal, A. Zamader, V. Nagayach, D. Dolui, A. Q. Mir and A. Dutta, *ACS Catal.*, 2019, **9**, 2334–2344.
11 L. A. Berben and J. C. Peters, *Chem. Commun.*, 2010, **46**, 398–400.
12 B. D. Stubbert, J. C. Peters and H. B. Gray, *J. Am. Chem. Soc.*, 2011, **133**, 18070–18073.
13 Y. Sun, J. P. Bigi, N. A. Piro, M. L. Tang, J. R. Long and C. J. Chang, *J. Am. Chem. Soc.*, 2011, **133**, 9212–9215.
14 S. Varma, C. E. Castillo, T. Stoll, J. Fortage, A. G. Blackman, F. Molton, A. Deronzier and M.-N. Collomb, *Phys. Chem. Chem. Phys.*, 2013, **15**, 17544–17552.
15 W. M. Singh, T. Baine, S. Kudo, S. Tian, X. A. N. Ma, H. Zhou, N. J. DeYonker, T. C. Pham, J. C. Bollinger, D. L. Baker, B. Yan, C. E. Webster and X. Zhao, *Angew. Chem. Int. Ed.*, 2012, **51**, 5941–5944.
16 C. C. L. McCrory, C. Uyeda and J. C. Peters, *J. Am. Chem. Soc.*, 2012, **134**, 3164–3170.
17 R. Zhang and J. J. Warren, *ChemSusChem*, 2021, **14**, 293–302.
18 J.-W. Wang, K. Yamauchi, H.-H. Huang, J.-K. Sun, Z.-M. Luo, D.-C. Zhong, T.-B. Lu and K. Sakai, *Angew. Chem. Int. Ed.*, 2019, **58**, 10923–10927.
19 V. Firpo, J. M. Le, V. Pavone, A. Lombardi and K. L. Bren, *Chem. Sci.*, 2018, **9**, 8582–8589.
20 B. Kandemir, S. Chakraborty, Y. Guo and K. L. Bren, *Inorg. Chem.*, 2016, **55**, 467–477.
21 B. Kandemir, L. Kubie, Y. Guo, B. Sheldon and K. L. Bren, *Inorg. Chem.*, 2016, **55**, 1355–1357.
22 F. Lakadamyali, M. Kato, N. M. Muresan and E. Reisner, *Angew. Chem. Int. Ed.*, 2012, **51**, 9381–9384.
23 J. G. Kleingardner, B. Kandemir and K. L. Bren, *J. Am. Chem. Soc.*, 2014, **136**, 4–7.
24 D. Dolui, S. Das, J. Bharti, S. Kumar, P. Kumar and A. Dutta, *Cell Rep. Phys. Sci.*, 2020, **1**, 100007.
25 D. Dolui, S. Khandelwal, A. Shaik, D. Gaat, V. Thiruvenkatam and A. Dutta, *ACS Catal.*, 2019, **9**, 10115–10125.
26 C.-L. Wang, H. Yang, J. Du and S.-Z. Zhan, *Appl. Organomet. Chem.*, 2022, **36**, e6453.